PHYSICAL REVIEW C VOLUME 7, NUMBER 4 APRIL 1973

Experimental Measurements of the $^{12}C + ^{12}C$ Nuclear Reactions at Low Energies

Michael G. Mazarakis* and William E. Stephens
Physics Department, University of Pennsylvania, Philadelphia, Pennsylvania 19104†
(Received 21 October 1972)

The nuclear reactions $^{12}C(^{12}C,\alpha)^{20}Ne$ and $^{12}C(^{12}C,p)^{23}Na$ have been observed from 5-MeV down to 2.45-MeV center-of-mass energy. Angular distributions and energy distributions of the protons and α particles were analyzed to obtain the total cross sections and other nuclear information. The Coulomb and angular momentum barrier penetrability was factored out to elucidate the intermediate resonance structure in the nuclear factor $\tilde{S}$. The observed rise in the nuclear factor at the lowest energies may be interpreted as "absorption under the barrier" as proposed by Michaud and Vogt. The importance of these reactions for the carbon burning era of nucleosynthesis and energy generation in the later evolution of stars is mentioned and reaction rates are estimated for various burning temperatures.

INTRODUCTION

In the calculations of energy generation and nucleosynthesis in the interior of stars, it is commonly understood that hydrogen fusion reactions lead to helium, and the triple helium reaction then generates carbon. Depending on the astrophysical environment, α captures further lead to ^{16}O and ^{20}Ne in various amounts. Significant amounts of carbon are estimated to be available in the cores of stars of medium mass. Furthermore, the $^{12}C + ^{12}C$ reactions have an appreciably lower Coulomb barrier and hence larger reaction cross section than $^{12}C + ^{16}O$ and $^{16}O + ^{16}O$ or ^{20}Ne reactions.[1] Consequently calculation of the later stages of stellar evolution involve the details of the carbon-burning reactions.

Although early calculations were made for constant temperature carbon burning,[2] it was soon recognized that neutrino losses would necessitate higher burning temperatures if not explosive burning.[3] The range of effective temperatures considered has ranged from 0.3 to 1.9×10^9 °K[4] corresponding to center-of-mass energies of 1 to 3.5 MeV.

Early calculations utilized nuclear data from similar reactions[2] and extrapolation using Coulomb barrier penetration to estimate pertinent $^{12}C + ^{12}C$ reaction rates.[5] The early experiments on $^{12}C + ^{12}C$ were performed with the Chalk River tandem accelerator and reported cross sections down to 5-MeV center-of-mass energy.[6] At the California Institute of Technology (CIT), the measurements were extended down to 3.4 MeV[7] and we have gone down to 2.45 MeV.

Our results were reported first in abstracts,[8] described in a thesis[9] and summarized in a letter to the *Astrophysical Journal*.[10]

APPARATUS

Carbon positive ions generated in a duoplasmatron ion source in a mixture of 25% methane and 75% helium were converted to negative ions by charge exchange in lithium vapor in the adder canal and accelerated in the University of Pennsylvania EN tandem accelerator. The beam was analyzed in the deflection magnet calibrated against $^2D(^{12}C,p_0)^{13}C$ with the proton energy determined in solid-state detectors which were in turn calibrated with an ^{241}Am α source. The C^{++} ions were stripped to an average charge state of 4^+ in passing through the carbon foil target and collected in a Faraday cup where their charge indicated 0.5 to 1.5 μA. This measurement of the beam current was not used for calculating cross sections. Instead, elastically scattered carbon nuclei were individually counted in a solid-state detector monitor at 45°. Using the Mott scattering cross section and the various geometric solid angles, the magnitude of the beam intensity was determined absolutely.

Silicon surface-barrier detectors made from millimeter thick 8200-Ω cm resistivity n-type silicon were placed close to the target in the scattering chamber[11] and arranged at angles of 20, 40, 60, and 80° to the beam. (These can be shifted 10° to give 30, 50, 70, and 90°.) These detectors were protected from the large fluxes of elastically scattered carbon ions by thin nickel foils whose thickness was chosen to completely stop the carbon ions and let most of the α particles and protons through. These foils limited the detection to protons and α particles above certain minimum energies which, however, were below the limits set by a large background of recoil protons and deuterons from the ubiquitous hydrogen contamination in the tar-

get. Figure 1 shows typical energy spectra of the reaction particles. The identification of the various groups was made by calculation of the laboratory energies from knowledge of the energy levels involved in the reactions (see Fig. 2) with corrections for target thickness, angle, and energy absorption in the foils. These identifications were checked by interposing a temporary additional nickel foil in front of the detectors to lower the α group energies appreciably more than the proton groups.

The targets were self-supporting foils evaporated from high-purity graphite and were 30 $\mu g/cm^2$ for most of the runs. For center-of-mass energies of 2.75 and 2.63 MeV the foils were 53 $\mu g/cm^2$, while at the lowest-energy run the foil was 65 $\mu g/cm^2$. The target thicknesses were measured by

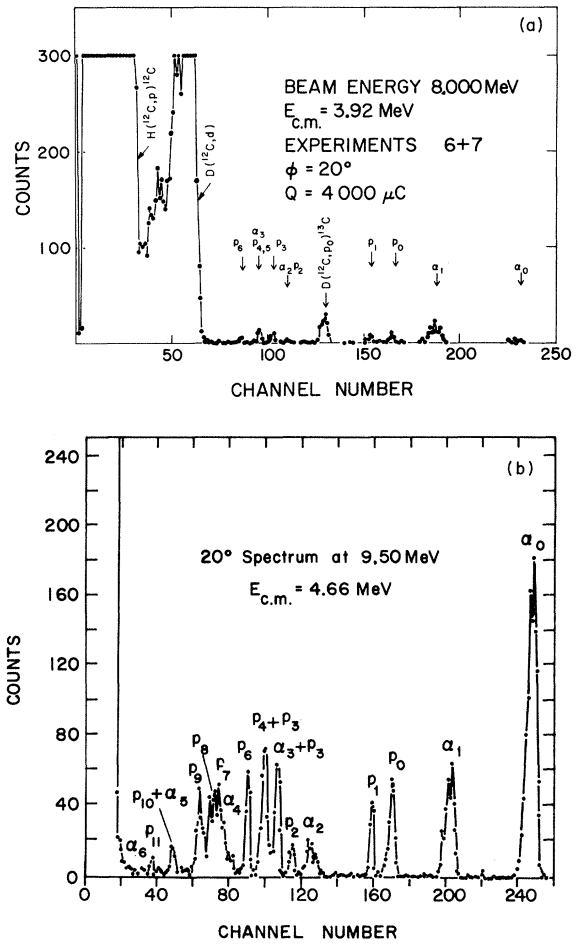

FIG. 1. Particle counts per analyzer channel. (a) Particle energy spectrum at 20° at 3.92-MeV center-of-mass energy. Peaks are identified in terms of $^{12}C(^{12}C,\alpha_i)^{20}Ne^*$ and $^{12}C(^{12}C,p_j)^{23}Na^*$; and the contamination recoils and $D(^{12}C,p_0)^{13}C$. (b) Similar spectrum at 20° and 4.66-MeV center-of-mass energy. See Fig. 2 for energy levels.

observing the loss of energy by ^{241}Am α particles in passing through the target. Corrections were then calculated for the energies of the carbon ions and α particles and protons at the center of the foil. At the lower energies it is necessary to correct for the nonlinear effects of the exponential dropoff of cross section in the target itself. The importance of making this correction was kindly brought to our attention by Professor William Fowler to whom we express our appreciation.

The signals from each of the detectors were separately gated into 256 channels of a 4096-channel analyzer. Corrections were made for counting losses in the multichannel analyzer.

EXPERIMENT

Angular distributions such as are shown in Fig. 3 were determined for each group of particles after the spectra from several runs were transformed into the center-of-mass system and summed. These angular distributions were fitted with even-order Legendre polynomials to order $l = 12$ and integrated to give the cross section for each particle group as identified in Fig. 2. These results are tabulated in Table I.

The total cross section for the charged particle exit channels are summarized in Table II and shown in Fig. 4. In order to see more clearly the strictly nuclear variation, it is convenient to separate out the steeply falling penetration probability of the Coulomb and angular momentum barrier. This is most conveniently approximated by the following simple expression for the cross section:

$$\sigma = \tilde{S}E^{-1}\exp-(2\pi\eta + gE)\,.$$

Here $\tilde{S}$ is the nuclear factor, E is the center-of-mass energy, g is the size factor $\frac{1}{3}(mR_0^3/2Z_1Z_2)^{1/2}$, η is the Gamow term $Z_1Z_2e^2/\hbar v$ with v the relative velocity, R_0 the nuclear separation, and m is the reduced mass. For the $^{12}C + ^{12}C$ reaction a standard formula is[7]

$$\sigma = \tilde{S}E^{-1}\exp-(87.21/\sqrt{E} + 0.46E)$$

The nuclear factor $\tilde{S}$ for the $^{12}C + ^{12}C$ results is given in Fig. 5.

ANALYSIS

The nuclear factor $\tilde{S}$ as shown in Fig. 5 as a function of energy exhibits a number of apparent resonances. Several of these (at 5.6 and 6 MeV) were originally interpreted as quasimolecular states.[12] Such an interpretation, even if correct, cannot be extended to the lower energy states because of inappropriate energy locations.[13] Again, these resonances are not Ericson fluctuations (i.e., statistical fluctuations of the compound nu-

TABLE I. Partial cross sections of the $^{12}C(^{12}C, \alpha)^{24}Ne$ and $^{12}C(^{12}C, p)^{23}Na$ reactions in μb.

Energy	Groups			α				Protons								
(MeV)	α_0	α_1	α_2	α_3	$\alpha_{4,5}$	α_6	α_7	p_0	p_1	p_2	p_3	$p_{4,5}$	p_6	p_7	$p_{8,9}$	p_{10}
2.45	0.0004	0.002	0.0007					0.0007	0.0003	0.0008	0.001	0.001	0.001			
2.63	0.006	0.005	0.005					0.001	0.003	0.004	0.006	0.010	0.006			
2.75	0.012	0.017	0.009	0.003				0.011	0.007	0.018	0.004	0.013	0.010			
2.92	0.025	0.053	0.024	0.034				0.014	0.037	0.017	0.027	0.021	0.017	0.029	0.055	
3.04	0.029	0.260	0.023	0.086				0.057	0.058	0.056	0.028	0.046	0.048	0.029	0.052	
3.17	0.080	0.300	0.031	0.055	0.060			0.120	0.084	0.074	0.045	0.070	0.036	0.150	0.180	
3.29	0.33	0.64	0.11	0.17				0.31	0.41	0.21	0.27	0.21	0.08	0.09		
3.42	1.80	0.73	0.22	0.24	0.27			0.70	0.54	0.40	0.44	0.34	0.38	0.22	0.40	
3.54	0.75	3.0	0.60	0.64	0.38			0.81	0.70	0.82	1.1	1.3	0.59	0.31	0.55	0.73
3.67	2.2	8.0	0.65	0.82	0.84			1.6	2.6	0.76	0.92	0.86	0.70	0.70	1.2	0.30
3.79	6.2	9.0	0.61	0.85	1.3			2.0	3.2	0.85	1.1	1.2	1.0	1.1	1.9	0.08
3.92	10	15	2.3	2.3	3.4			17	4.6	3.6	7.4	5.0	2.6	2.8	4.9	0.2
4.04	17	26	6.8	2.3	5.9			14	13	7.0	25	16	3.2	4.8	8.5	2.4
4.17	89	160	21	9.1	29	1		68	64	12	81	37	27	23	41	27
4.29	88	220	19	10	37	5.4		45	59	23	20	63	18	30	53	30
4.42	140	250	36	34	110	5.5		69	66	32	29	170	110	90	160	68
4.54	350	130	51	28	150	5.5		100	78	46	29	280	64	120	220	38
4.66	430	370	89	60	170	10	3.1	250	170	44	61	120	170	380	←	59
4.79	76	1430	260	150	530	16	11	590	650	150	180	540	140	1210	←	150
4.91	840	2300	580	210	900	58	40	520	1090	310	570	540	400	2030	←	320

TABLE II. Total cross sections and nuclear factors of the $^{12}C(^{12}C, \alpha)^{20}Ne$, $^{12}C(^{12}C, p)^{23}Na$, and $^{12}C(^{12}C, n)^{23}Mg$ reactions. The σ_n are those given by Patterson, Winkier, and Zaidins (Ref. 7). For the lower energies (threshold, 2.6 MeV), σ_{tot} contains extrapolated values of σ_n.

c.m. energy (MeV)	σ_α (mb)	Error (%)	σ_p (mb)	Error (%)	σ_n (mb)	Error (%)	σ_{tot} (mb)	Error (%)	$\tilde{S}$ (10^{16} MeV b)
2.45	0.000 003	50	0.000 005	40	···	···	0.000 008	30	7.3
2.63	0.000 016	35	0.000 030	30	···	···	0.000 05	24	8.6
2.75	0.000 04	29	0.000 06	24	···	···	0.000 11	19	6.5
2.92	0.000 14	20	0.000 22	23	···	···	0.000 36	16	5.9
3.04	0.000 40	17	0.000 37	15	···	···	0.0008	14	4.9
3.17	0.000 53	13	0.000 77	10	···	···	0.0013	11	3.4
3.29	0.0012	10	0.0016	9	···	···	0.0029	9	3.2
3.42	0.0032	9	0.0034	9	···	···	0.0068	8	3.4
3.54	0.0054	8	0.0063	8	···	···	0.012	8	2.9
3.67	0.012	8	0.0096	9	···	···	0.022	8	2.7
3.79	0.018	8	0.012	8	···	···	0.031	7	1.9
3.92	0.033	7	0.048	7	···	···	0.083	7	2.7
4.04	0.057	7	0.094	7	···	···	0.15	7	2.8
4.17	0.30	7	0.39	7	0.006	30	0.70	7	7.2
4.29	0.38	7	0.35	7	0.012	30	0.74	7	4.5
4.42	0.58	7	0.80	7	0.026	20	1.4	7	5.1
4.54	0.72	7	0.99	7	0.059	15	1.8	7	3.9
4.66	1.12	7	1.27	7	0.12	15	2.5	7	3.5
4.79	2.5	7	3.7	7	0.25	15	6.4	7	5.8
4.91	4.9	7	6.1	7	0.44	15	11.4	7	6.7

TABLE III. Carbon-carbon reaction rate at various temperatures (cm^3/sec g).

	T_9 =	3	2	1	0.6	0.3
Assuming resonance at 2.5 MeV		$\frac{2}{3}R_3$	$\frac{2}{3}R_2$	$\frac{4}{5}R_2$	$\frac{1}{2}R_{0.6}$	$\frac{1}{2}R_{0.3}$
Reeve's (1966) extrapolation	R_T =	1.33	8.78×10^{-4}	1.14×10^{-10}	4.61×10^{-17}	6.5×10^{-28}
Absorption under barrier		$\frac{2}{3}R_3$	$\frac{5}{7}R_2$	$\frac{5}{3}R_1$	$\frac{10}{3}R_{0.6}$	$8R_{0.3}$

cleus), since the α and proton excitation functions both rise at the 4.17- and 4.9-MeV peaks.

Looking further, we can recall that reasonable optical potentials give level separation between single-particle resonances of greater than several MeV, while compound nuclear states of ^{24}Mg at these excitation energies would be expected to have level spacings of a few keV. Consequently, intermediate structure resonances with possible spacings of the order of 0.5 MeV have been suggested as an explanation of the 4-MeV peaks.

As shown in the analysis of the α-particle angular distributions exhibited in Fig. 3, the resonances at both 4.17 and 4.9 MeV are likely to be associated with a spin of 4 (analysis from the α_0 angular distributions give $l=0,2,4$ while that from α_1 gives $l\geq4$). There may, of course, be a continuum of compound nuclear states of other spin superimposed on these main resonances.

The partial cross sections given in Table I can be used to derive the branching ratios to the various excited states of the resultant nucleus. Figure 6(a)

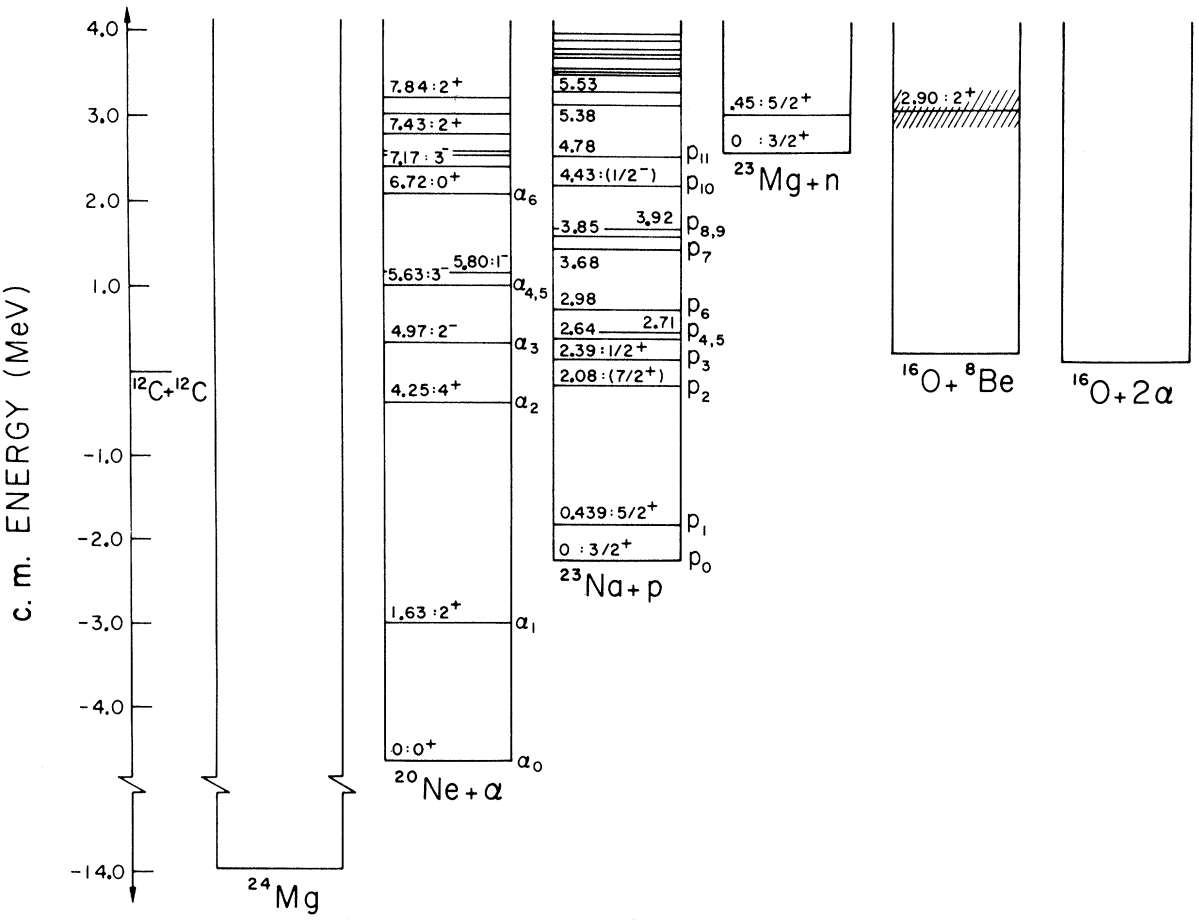

FIG. 2. Energy-level diagrams for the $^{12}C+^{12}C$ reactions showing levels in ^{20}Ne and ^{23}Na with the particle groups identified.

shows the branching ratio of the α particles emitted into the fourth and fifth excited states of ^{20}Ne (3^- and 1^-) compared to the total α emission. Figure 6(b) shows the same ratio for the sixth excited state of ^{20}Ne (0^+). Also on these figures are plotted the calculations of Michaud and Vogt[14] based on the statistical theory of compound nuclear reactions. The solid line is for a radius $R_0 = 5$ fm of the optical potential of the ^{20}Ne + α channel while the dashed curve is for $R_0 = 4.5$ fm. It will be noted that the observed branching ratios for the combined transitions to 3^- and 1^- states do not decrease at low energies as predicted, while the ratio for the 0^+ level does. This has been interpreted by Michaud and Vogt as evidence for an intermediate structure model based on an α-particle cluster picture of ^{12}C. They point out that the reduced widths for ^{16}O + α of the 1^-, 5.78-MeV and the 0^+, 6.72-MeV states in ^{20}Ne are both close to the single-particle reduced width while the reduced width for the 3^-, 5.62-MeV state is less than one hundreth that observed in the ^{16}O + α reaction.[15] The

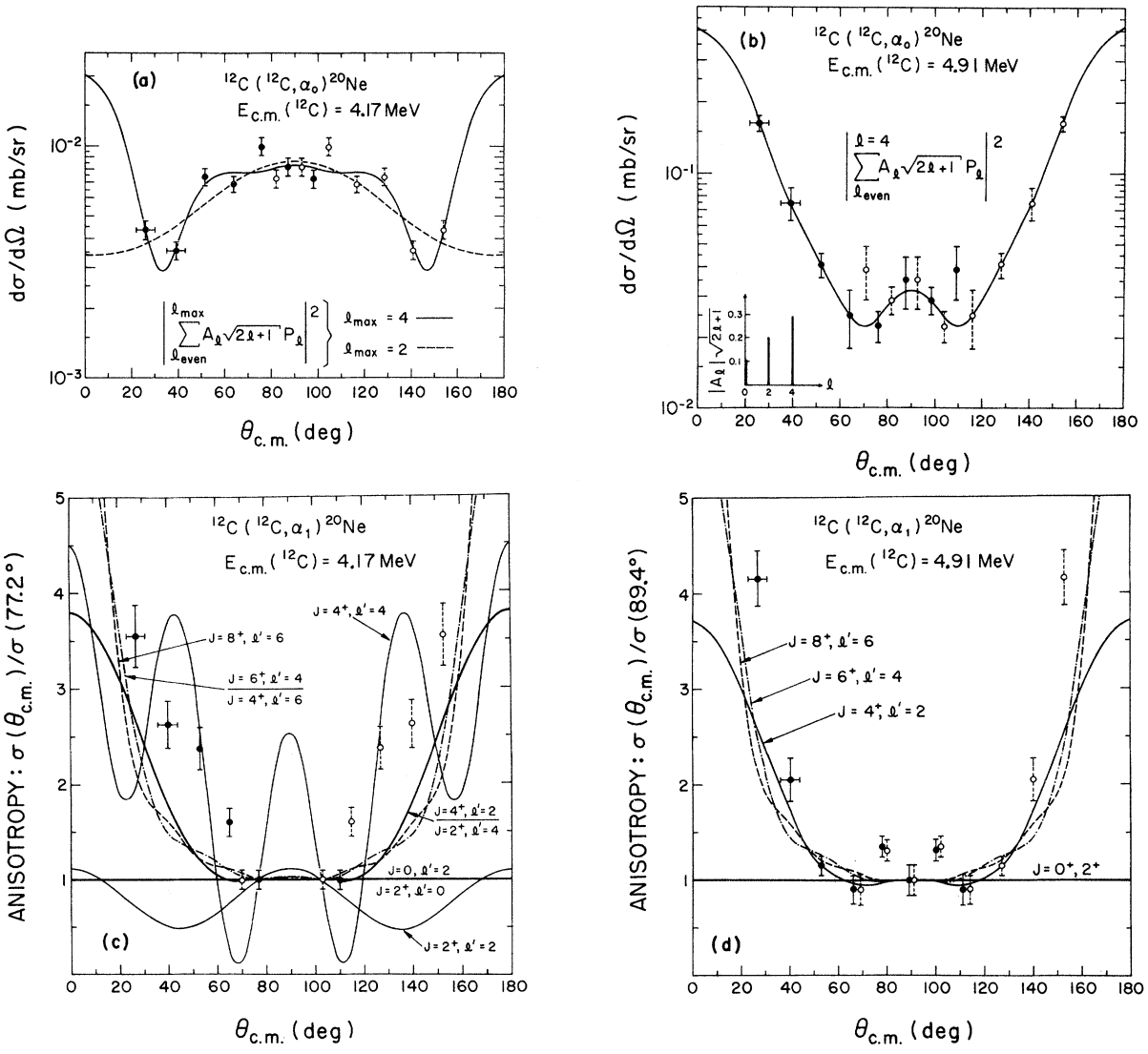

FIG. 3. Partial cross sections as a function of center-of-mass angle for α groups in the ^{12}C(^{12}C,α)^{20}Ne reaction. (a) α_0 group at 4.17-MeV center-of-mass energy; (b) α_0 group at 4.91 MeV; (c) α_1 group at 4.17 MeV; (d) α_1 group at 4.91 MeV. The circle points are inferred assuming symmetry. The curves represent calculated values for the indicated assumptions on angular momentum.

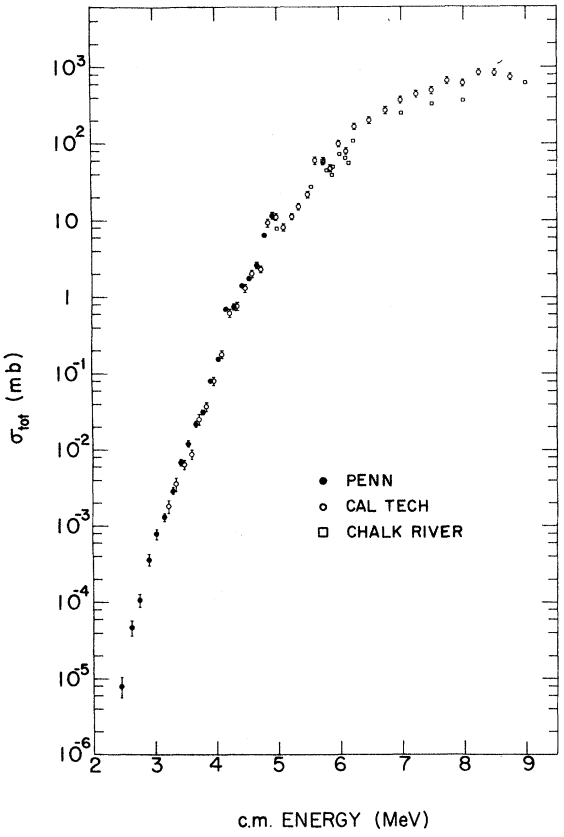

FIG. 4. Total reaction cross section in mb as a function of center-of-mass energy in MeV.

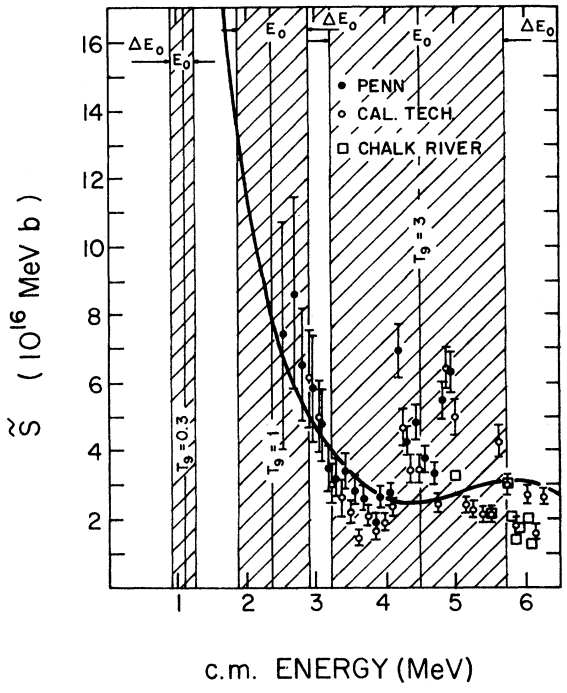

FIG. 5. Nuclear factor $\tilde{S}$ in units of 10^{16} MeV b as a function of center-of-mass energy in MeV. The curve represents the calculations of Michaud (Ref. 18) for an optical-model calculation using a potential from the α-α interaction and illustrating penetration under the barrier. The hatched areas illustrate the regions of importance in carbon burning at temperatures of T_9 = 0.3, 1, and 3.

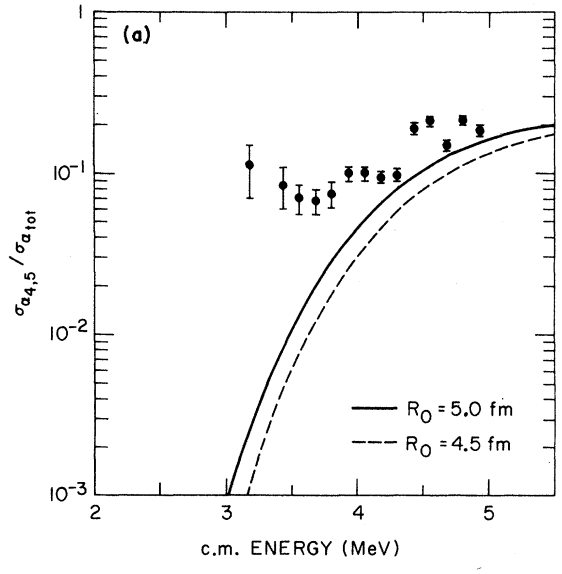

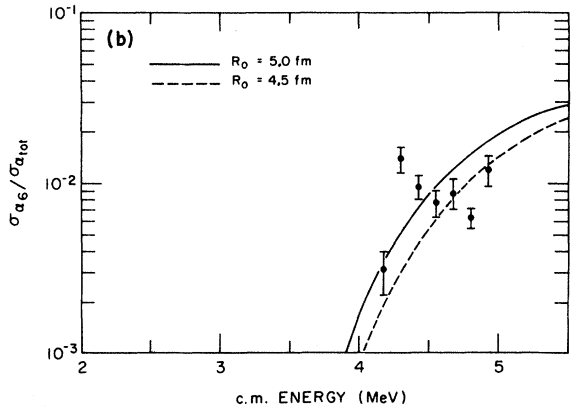

FIG. 6. Branching ratios as a function of center-of-mass energy. (a) For α particles to the fourth and fifth excited states of ^{20}Ne. (b) α particles to the sixth excited state of ^{20}Ne. Curves from calculations using the statistical model.

inference is that since the 3^- state has such a low reduced width, the wave functions for the oxygen-16 ground state plus one α particle have relatively small overlap with that for the 3^- ^{20}Ne. Therefore it is possible that the overlap of the 3^- level would be larger with respect to a carbon core plus two α particles. If that were so, direct reaction processes involving ^{12}C plus a cluster of α particles would contribute to the excitation of the 3^- level and the branching ratio leading to the 3^- level would be larger than expected statistically, and in agreement with that observed.

The rise in the nuclear factor at energies below 3 MeV is an interesting result of the present experiment. It is important to understand the nature of this rise because such understanding is crucial for extrapolation of the cross section to the lower energies which are important for the astrophysical problem of carbon burning. The three obvious interpretations of such an increase in the nuclear factor are: (1) a giant resonance (optical-model single-particle type resonance), (2) an intermediate state, and (3) an aggregation of compound nuclear states. As mentioned before, compound nuclear states are expected to have spacings and widths of tens of keV or less. Nevertheless, fortuitous aggregation and overlapping of a number of such levels could conceivably give rise to the observed strength. This possibility is emphasized by recent observations in the ^{16}O(^{12}C, α)^{24}Mg reaction that three compound-nuclear-type resonances are strongly excited in ^{24}Mg at 16.30, 16.56, and 16.84 MeV in close coincidence with the center-of-mass energy of 2.4 to 2.9 MeV in the ^{12}C + ^{12}C energy scale. These states in ^{24}Mg have been found

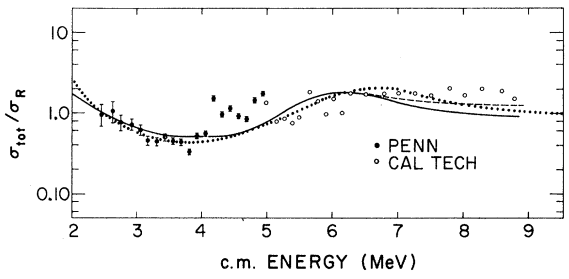

FIG. 7. The total cross section of the ^{12}C + ^{12}C reactions in units of Reeves's extrapolation as a function of center-of-mass energy. This is equivalent to exhibiting the energy variation of the nuclear factor $\tilde{S}$. The dotted curve shows the results of calculations of Michaud and Vogt using an optical model with potential $V_0 = 23$ MeV, $W_0 = 0.2E$ MeV, $R_0 = 6$ fm, and $a = 0.5$ fm. The solid curve represents the calculations of Michaud and Vogt using an optical model with soft-core potential from α-α interaction, $W_0 = 1$ MeV, $R_I = 6$ fm, and $\alpha = 0.55$ fm. The dashed curve has $W_0 = [1 + (E - 6)/5]$ MeV.

to be of high spin ($J = 8, 9$).[16] The branching ratios of α_1/α_0 and α_2/α_1 as observed in our measurements are not inconsistent within the inevitable uncertainties with those observed for these ^{24}Mg states. Nevertheless, it would seem unlikely that the strength observed in the ^{12}C + ^{12}C cross section would be coincidentally supplied by compound nuclear states. Similar comments apply to an interpretation as an intermediate state. The width inferred from the observations is considerably larger and the strength greater than would be predicted from intermediate structure.

Michaud and Vogt[14] have investigated a number of optical-model potentials to fit the observed ^{12}C + ^{12}C cross-section variation with intermediate structure averaged out. As their paper points out, several sets of assumptions predict cross-section curves not too different from the experimental results. These include:

(1) A Woods-Saxon potential with $V_0 = 23$ MeV, $W_0 = 0.2E$, $R_0 = 6.0$ fm, and $a = 0.5$ fm.

(2) A Woods-Saxon potential with $V_0 = 85.8$ MeV, $W_0 = 0.2E$, $R_0 = 5.7$ fm, $a_R = 0.5$ fm, and $\alpha_I = 0.6$ fm.

(3) A soft-core potential from an α-cluster model for ^{12}C with $W_0 = 1$ MeV, $R_I = 6$ fm, and $a = 0.55$ fm.

The first of these optical-model potentials fits the observed data by producing giant resonances at $E = 2$ MeV and $E = 6$ MeV. The fit is shown in Fig. 7. The third potential is derived from an α-cluster model of the carbon nucleus and produces only one giant resonance at $E = 6$ MeV. The rise at lower energies is provided by absorption under the barrier as shown in Fig. 7.

This absorption under the barrier is an interesting new physical concept and is appealing in its simplicity.[17] It of course depends on the potential extending appreciably farther out than square-well potentials. In a more recent paper, Michaud[18] shows that such a soft repulsive core of the form $V_R e^{-cr^2}$ added to a Woods-Saxon potential is necessary to adequately interpret the data from ^{12}C + ^{12}C, ^{16}O + ^{16}O as well as ^{16}O + ^{12}C in a consistent fashion. His best fit to our experimental data is obtained with the parameters:

$$V_0 = 13 \text{ MeV}, \quad R_0 = 6.2 \text{ fm}, \quad V_R = 100 \text{ MeV},$$
$$W_0 = 0.22E, \quad a = 0.55 \text{ fm}, \quad c = 0.1 \text{ fm}^{-2}.$$

The low energy part of that fit is shown in Fig. 5 where the solid curve is from Michaud's calculations.

While more measurements particularly at lower energies would be desirable to understand the nuclear phenomena, the smallness of the reaction cross sections involved due to the Coulomb barrier makes further measurements at lower energies very difficult, if not impossible, with present ex-

perimental techniques. Consequently, it will be useful to present estimates based on extrapolations of the present data to lower energies. Two reasonable extremes of the present knowledge suggest extrapolation based on (1) the Michaud and Vogt α-cluster model potential including absorption under the barrier or (2) a possible resonance near 2.5 MeV. These assumptions give extrapolations which can be expressed in terms of factors that compare them to the older standard extrapolation of Reeves. Such factors are shown in Table III for the reaction rate R_T for several temperatures. The reaction rate at a given temperature T is defined by $R_T = N_A \langle \sigma v \rangle$ in units of $cm^3/sec\ g$, where N_A is Avogadro's number and $\langle \sigma v \rangle$ is the mean product of reaction cross section and relative velocity at the given temperature.[19] It can be seen that the Michaud-Vogt α model leads to reaction rates considerably larger than the other extreme or the older commonly used values.

---

*Now at Physics Department, Rutgers University, New Brunswick, New Jersey.

†Work supported in part by the National Science Foundation.

[1]D. D. Clayton, in *Principles of Stellar Evaluation and Nucleosynthesis* (McGraw-Hill, New York, 1968), Chap. 5.

[2]H. Reeves and E. E. Salpeter, Phys. Rev. 116, 1505 (1959).

[3]W. A. Fowler and F. Hoyle, Astrophys. J. Suppl. Ser. 9, No. 91, 201 (1964).

[4]W. D. Arnett and J. W. Truran, Astrophys. J. 157, 339 (1969); W. D. Arnett, *ibid.* 157, 1369 (1969); Z. Barbat, J. C. Wheeler, J. R. Buchler, *ibid.* 171, 651 (1972); W. D. Arnett, Astrophys. Space Sci. 5, 180 (1969); and Astrophys. J. 162, 349 (1970).

[5]H. Reeves, Astrophys. J. 146, 447 (1966).

[6]E. Almquist, J. A. Kuehner, D. McPherson, and W. E. Vogt, Phys. Rev. 136, B1384 (1964).

[7]J. R. Patterson, H. Winkler, and C. S. Zaidins, Astrophys. J. 157, 367 (1969).

[8]M. G. Mazarakis and W. E. Stephens, Bull. Am. Phys. Soc. 15, 629 (1970); M. G. Mazarakis, G. O.DeBolt, Jr., and W. E. Stephens, *ibid.* 16, 600 (1971).

[9]M. G. Mazarakis, Ph.D. thesis, University of Pennsylvania, 1971 (unpublished).

[10]M. Mazarakis and W. Stephens, Astrophys. J. 171, 197 (1972).

[11]R. W. Zurmuhle, Nucl. Instr. Methods 36, 168 (1965).

[12]E. Vogt and H. McManus, Phys. Rev. Letters 4, 518 (1960).

[13]H. J. Fink, W. Scheid, and W. Greiner, Nucl. Phys. A188, 259 (1972).

[14]G. J. Michaud and E. W. Vogt, Phys. Rev. C 5, 350 (1972).

[15]C. Van der Leun *et al.*, Phys. Letters 18, 134 (1965).

[16]D. P. Balamuth, J. E. Holden, J. W. Noé, and R. W. Zurmuhle, Phys. Letters 26, 1271 (1971); R. W. Zurmühle, D. P. Balamuth, L. K. Fifield, and J. W. Noé, Phys. Rev. Letters 29, 795 (1972).

[17]G. Michaud, L. Scherk, and E. Vogt, Phys. Rev. C 1, 864 (1970).

[18]G. Michaud, Astrophys. J. 175, 751 (1972).

[19]W. A. Fowler, G. R. Caughlan, and B. A. Zimmerman, Ann. Rev. Astron. Astrophys. 5, 525 (1967).